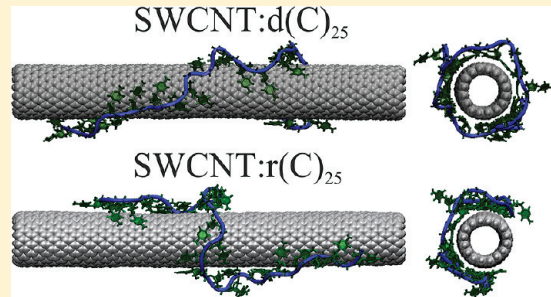


Peculiarities of Homooligonucleotides Wrapping around Carbon Nanotubes: Molecular Dynamics Modeling

Maxim V. Karachevtsev and Victor A. Karachevtsev*

B. Verkin Institute for Low Temperature Physics and Engineering, National Academy of Sciences of Ukraine, 47, Lenin Ave., 61103 Kharkov, Ukraine

ABSTRACT: Spontaneous adsorption of homooligonucleotides dC_{25} , dT_{25} , dG_{25} , and dA_{25} on the surface of the carbon nanotube (16,0) has been simulated by the molecular dynamics method. It was demonstrated that the rate of pyrimidine oligonucleotide wrapping around the nanotube is higher than that of purine ones which do not form a complete pitch even after the maximum simulation time (50 ns). This behavior can be explained by a stronger self-stacking between the purines than pyrimidines, which prevents the reorientation of the polymer required for the acquisition of a more energetically favored conformation on the nanotube. Estimations obtained from modeling allowed to establish the oligonucleotide row which demonstrates decreasing interaction energies between oligonucleotides and the carbon nanotube: $d(T)_{25} > d(C)_{25} > d(A)_{25} \approx d(G)_{25}$. It was shown that the temperature growth increases the rate of oligonucleotides to reach the maximum binding energy mainly due to the destruction of nitrogen base self-stacking. Ribonucleic oligonucleotides $r(C)_{25}$, $r(A)_{25}$, and $r(G)_{25}$ do not make a pitch around the nanotube for 50 ns. The presence of the additional hydroxyl group in ribose restricts the conformational flexibility of ribonucleic oligonucleotides in comparison with their deoxy analogues and this reduces the possibility of rapid occupation of the stable conformation on the nanotube surface.



1. INTRODUCTION

Biomolecules interacting with inorganic nanostructures form different nanohybrids with unusual multifunctional properties, which have a wide spectrum of applications in nanomedicine, biosensing, nanoelectronics, environmental safety, and so on. DNA (the main molecule of life) creates a hybrid with a carbon single-walled carbon nanotube (SWCNT) in water, which is a subject of intensive current interest.^{1–8} SWCNTs have a set of unique physical/chemical properties, for example, mechanical stiffness, and unusual photophysical properties. Besides, nanotubes exhibit a versatile electronic nature which leads to modern molecular electronics (see, for example, the review (ref 9) or book (ref 10)). In spite of the essential difference in single-stranded DNA (ssDNA) and nanotube structures, ssDNA is a flexible, amphiphilic biopolymer whereas SWCNT is stiff hydrophobic nanorod; they form a stable hybrid in water. It is obvious that properties of these two nanostructures supplement each other, and, as a result, a hybrid with specific structural features is formed. Due to its helical structure, DNA wraps tightly around the nanotube in water. As ssDNA in aqueous solution carries a negative charge in the chain and, as well, contains hydrophobic components, the stable hybrid with the tube is created when hydrophobic nitrogen bases are adsorbed to the nanotube surface via $\pi-\pi$ stacking, while the hydrophilic sugar–phosphate backbone is directed to water.^{1,2} ssDNA consisting of the sequence of four bases involves a set of polymers with slightly different physical properties (rigidity, thermostability etc.). It is reasonable to suppose that each polymer binds most effectively only to the

nanotube of a certain diameter. Thus, it should rely on the separation of nanotubes with certain chirality from the bulk material by choosing an appropriate DNA sequence.⁸ Besides the nanotube solubilization and separation by DNA, another very promising application for this hybrid is to determine the polymer sequence, using SWCNT, first, as a template to hold DNA in the stretched form and, then, DNA sensing through different electrical measurements, for example, with STM¹¹ or a carbon nanotube field-effect transistor.¹² As well, the development of a genosensor with optical detection, using SWCNTs for this purpose, is a very encouraging approach¹³ too.

Last time, molecular dynamics (MD) was intensively exploited to clarify self-assembly mechanisms characterizing SWCNT:DNA, to determine the hybrid structure and to evaluate the interaction energy.^{2,7,14–25} Very important experimental parameters including temperature, pressure, and environment (e.g., water) are taken into account in this powerful computational method. These useful parameters applied in modeling give a certain advantage to MD over ab initio calculations which can characterize only small molecules or systems. However, it should be noted that the last method provides high accuracy in determining of the structure, spectral parameters, and interaction energies. This modeling approach is especially appropriate for biophysical systems²⁶ and nanohybrids. MD significance increases manifold

Received: March 21, 2011

Revised: June 17, 2011

Published: June 17, 2011

when the experimental realization is complicated or impossible at all.

MD simulations carried out by Gao et al.^{14,15} showed strong association of short SWCNT and ssDNA octamers in water, which are not only adsorbed to the outer tube surface but can also insert into the nanotube.

Lu et al.¹⁶ modeled a periodic array of SWCNTs in contact with DNA, emphasizing on the electron transport in both the components, and, a result, this nanosystem was proposed as a very sensitive nanoscale electronic device for ultrafast DNA sequencing.

Using MD simulations, Manohar et al.¹⁷ demonstrated that the free energy upon the hybrid formation is determined by the adhesion between DNA bases and SWCNT, entropy of the DNA backbone, and electrostatic interactions between backbone charges. It was also revealed that the ionic strength of solution has a strong influence on SWCNT:DNA structure.

Earlier, Martin et al.²⁰ used replica exchange molecular dynamics (REMD) simulations to study the association of several ssDNA decamers ($d(T)_{10}$, $d(G)_{10}$, and $d(GT)_{10}$) with SWCNTs of different chiralities in the aqueous environment. They found that, after the fast adsorption onto the nanotube surface, oligonucleotides undergo a slow structural rearrangement. Population distribution maps were computed as a function of several local and global order parameters. It was shown that DNA in the hybrid acquires a number of distinct backbone geometries which depend both on DNA sequence and the nanotube diameter.

Exploring self-assembly mechanisms, R. Johnson et al.¹⁹ performed MD simulations to determine the structure and energetic properties of SWCNT:(14-base oligonucleotide) hybrid. They found that in aqueous solution short ssDNA near SWCNT undergoes a conformational change via the $\pi-\pi$ stacking interaction between nitrogen bases and the nanotube surface. This structure conformation enables the biopolymer to wrap spontaneously around SWCNT into compact right- or left-handed helices. Driving forces which provide the polymer helical wrapping are electrostatic and torsional interactions within the sugar-phosphate backbone. In a recent publication, these authors showed the entire ensemble of oligonucleotide conformations in the SWCNT:(GT)₇ hybrid.¹⁹ They calculated the free energy landscape and found the global minimum corresponding to a nonhelical loop structure of the polymer.²³ These authors computed also the base-SWCNT binding free energy for all four DNA bases in aqueous solution at room temperature and showed that this energy for purine bases prevail over pyrimidine ones.²⁴ Base-SWCNT binding is dominated by van der Waals (vdW) forces between the base and nanotube sidewall, while solvation and entropic effects play a relatively minor role.²⁴

A more complicated situation takes place with double-stranded DNA (dsDNA) when this polymer is adsorbed to the nanotube. Hydrophobic bases in the double helix are located inside and bound with H-bonds. Thus, the model based on ssDNA wrapping around SWCNT is inapplicable in this case. However, as follows from experimental observations, tubes form hybrids with dsDNA.^{22,27–30} It was demonstrated that SWCNTs can readily be dispersed by long salmon genomic dsDNA, and this gives hope that the nanotube solubilization will not be very expensive.²² It is assumed that the formation of SWCNT:dsDNA hybrids starts due to the interaction between the nanotube and untwisted ssDNA formed mainly at the polymer ends.²⁷ These untwisted regions are always presented in the polymer at room temperatures and are also formed after sonication (the common method used for the

hybrid preparation). These strands wrap around the tube and serve as an “anchor” for the whole polymer.

J. Johnson and Zhao¹⁸ reported on MD simulation of the dodecamer dsDNA binding to SWCNT in water. It was found that dsDNA does not wrap around the tube but rather attaches to the surface via its hydrophobic end groups. However, as the recent experimental study showed, the double polymer located on the nanotube splits with time,³¹ and then the single-stranded polymer wraps around the nanotube spontaneously. But this process is rather slow (it takes more than 1 month).

In spite of essential efforts of investigators studying physical properties of this nanobiohybrid, some questions (including a search for polymers which realize fast wrapping around the tube with maximal nanotube:DNA interactions and effective nanotube solubilization) have not been well understood up to now. As well, it should be added that the hybrid structure of SWCNT with a relatively long polymer has not been investigated properly yet. It was supposed that the structure of such a hybrid can be different from that of hybrids with short oligonucleotides. It was shown that a longer ssDNA is able to wrap around the nanotube in several layers.³² In the majority of simulations, the length of the oligonucleotide was lesser than 15 nucleotides. It should be added that in some cases a short DNA adsorbs to SWCNT in folded sections on the tube side rather than upon wrapping.³³

In this work, we performed MD simulation of relative long homooligonucleotide adsorption on the SWCNT surface. We did not try to find the global maximum of the interaction energy between the polymer and the nanotube, but rather we wanted to determine which of the synthetic oligonucleotides studied reaches rapidly the more energetically favored conformation on the nanotube surface as well as to know which one interacts more efficiently with tubes to provide the stable nanotube solubilization. The purposes pursued were to elucidate which polymer can provide the effective interaction with the tube surface, emphasizing the difference between purine and pyrimidine oligonucleotides in the wrapping process as well as to determine which polymer among deoxyribonucleotides or ribonucleotides are preferable in this process. Another aim of this study was to find out the temperature effect on the wrapping rate as well as to determine hybrid structures and the interaction energy. The choice of homooligonucleotides for studying the hybrid formation with the nanotube was based on extensive experimental information on these well-studied model systems, with the desire to avoid ambiguity in the result interpretation, appearing sometimes upon studying the heterogeneous base sequence. Besides, the substantial argument is relatively low costs of homopolynucleotides as this factor often becomes a stumbling block in the way of practical application.

2. MOLECULAR DYNAMICS SIMULATION

The formation of SWCNT hybrids with purine and pyrimidine homooligonucleotides was simulated by the molecular dynamics method. For this purpose the program package NAMD³⁴ was employed with Charmm27 force field parameter set.³⁵ Oligonucleotides used in simulations were 25 deoxyribonucleotides dC_{25} , dT_{25} , dG_{25} , and dA_{25} (in B-conformation) and ribonucleotides $r(C)_{25}$, $r(A)_{25}$, and $r(G)_{25}$ (in A-conformation). Modeling boxes were applied, the size of which was varied from $52 \text{ \AA} \times 66 \text{ \AA} \times 141 \text{ \AA}$ to $45 \text{ \AA} \times 59 \text{ \AA} \times 135 \text{ \AA}$. Nanobiohybrids were embedded in water (more than 10 300 H_2O molecules). For modeling, periodical boundary conditions were provided. In all the cases, SWCNT was

selected as a zigzag (16,0) nanotube. Its length and diameter were 11.0 and 1.25 nm, respectively.

Before starting simulation, the oligonucleotide was located near the nanotube surface. For neutralization of the charge on the sugar–phosphate backbone, 25 Na⁺ ions were added to each modeling system. Such systems were minimized during 1000 steps (with 1 fs time step) and then modeled during 50 ns (time step was also 1 fs). Essential structure transformation or changes in physical parameters were not observed during last 10 ns. In our

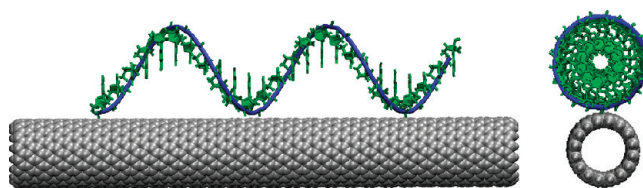


Figure 1. Snapshot of d(C)₂₅ structure and SWCNT (16,0) in the initial simulation step. Water molecules and Na⁺ counterions are removed for better visualization. The sugar–phosphate backbone is depicted by the blue solid curve.

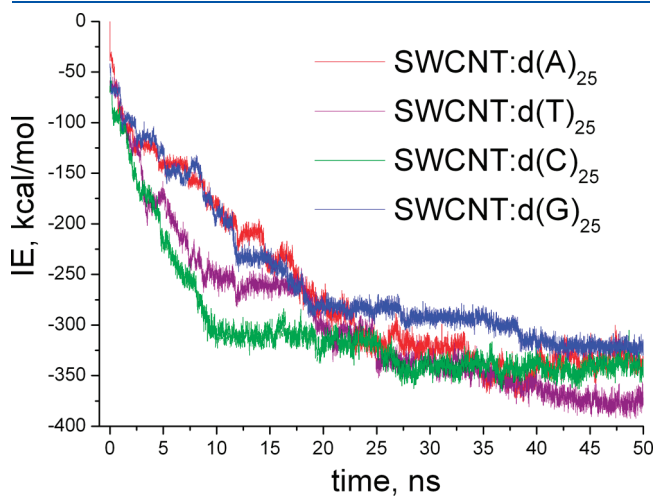


Figure 2. Dependence of interaction energy between SWCNT and d(C)₂₅, d(T)₂₅, d(A)₂₅, and d(G)₂₅ oligonucleotides on simulation time.

Table 1. Number of Nitrogen Bases of the Following Oligonucleotides: d(C)₂₅, d(T)₂₅, d(A)₂₅, and d(G)₂₅. Which Were in Stack with Tube Surface and Self-Stacked for Different Simulation Stages

time (ns)	type of nitrogen base stacking	d(C) ₂₅	d(T) ₂₅	d(A) ₂₅	d(G) ₂₅
0	self-stacking	25 cytosines	25 thymines	25 adenines	25 guanines
10	stacked with tube	18 cytosines	13 thymines	8 adenines	8 guanines
	self-stacking	2 (CC)	1 (TTT), 3 (TT), 1 loop	1 (AAAA), 1 (AAAA), 1 (AAA), 1 (AA), 2 loops	3 (GGGG), 2 (GG)
20	stacked with tube	18 cytosines, <i>a pitch was formed</i>	15 thymines	14 adenines	14 guanines
	self-stacking	3 (CC)	1 (TTT), 3 (TT), 1 loop	1 (AAAA), 3 (AA), 1 loop	2 (GGG), 3 (GG), 1 loop
30	stacked with tube	21 cytosines	18 thymines, <i>a pitch was formed</i>	16 adenines	14 guanines
	self-stacking	0	3 (TT)	1 (AAAA), 3 (AA), 1 loop	1 (GGGG), 2 (GGG), 1 (GG), 1 loop
40	stacked with tube	20 cytosines	20 thymines	16 adenines	15 guanines
	self-stacking	0	2 (TT)	1 (AAAA), 3 (AA), 1 loop	1 (GGG), 3 (GG), 1 loop
50	stacked with tube	21 cytosines	22 thymines	16 adenines	17 guanines
	self-stacking	0	1 (TT)	1 (AAAA), 2 (AA), 1 loop	1 (GGG), 3 (GG), 1 loop

simulations, NPT ensembles were used, and SWCNT atoms were uncharged. To speed up the process of spontaneous adsorption and to achieve the stable arrangement of oligonucleotides on the nanotube surface, the temperature in the simulation was taken as 343 K. The modeling pressure in the periodic box was 1 atm. Interaction energy was calculated by the NAMD Energy Plugin (Version 1.3) which was implemented in the VMD program package.³⁶ Water was not included into calculations of the interaction energy directly. As atoms of the nanotube were not charged, the electrostatic interaction was not taken into account in calculations of the energy of interactions between components of the hybrid. In such case, vdW interaction determined the binding energy of oligonucleotides with the nanotube.²⁴

3. RESULTS AND DISCUSSION

3.1. Peculiarities of Pyrimidine and Purine Oligonucleotide Adsorption on Carbon Nanotubes. In the initial step of the computer modeling, one deoxyribooligonucleotide selected from dC₂₅, dT₂₅, dG₂₅, and dA₂₅ raw in the self-ordering helical B-form³⁷ was located near the carbon nanotube surface, and then simulation started (Figure 1). In our simulation, the structure of the hybrid and the interaction energy between SWCNT and the selected oligonucleotide were controlled.

Figure 2 presents dependences of the nanotube:oligonucleotide interaction energy on simulation time for all the oligonucleotides. The gradual increase of the binding energy within 40 ns is common for all the dependences. Of special note is the very strong energy increase between components of SWCNT:dC₂₅ hybrid for which the magnitude of this interaction was more than 300 kcal/mol after the first 10 ns. In spite of the fastest rate of the binding energy increase, dC₂₅ did not make a pitch around the nanotube after the first 10 ns. Nevertheless, 18 cytosines were already in stacking with the tube surface, and only four bases were in self-stacking, forming two dimers (Table 1). Special attention was concentrated on the number of nitrogen bases stacked with the tube surface as this polymer component contacts with SWCNT directly and gives the basic contribution to the interaction energy.^{38,39} A nitrogen base is considered as stacked if more than half of pyrimidine or purine ring atoms are in van der Waals contact with the nanotube surface. The second oligonucleotide which demonstrates the high rate of achieving the stable conformation

on the tube surface is dT_{25} with 13 thymines stacked with the tube after 10 ns. The interaction energy of the purine oligonucleotides with the tube increases with significantly lower rate. Thus, after 10 ns only 8 adenines and 7 guanines were stacked with the nanotube surface.

During next 10 ns, dC_{25} is wrapped around the nanotube, completing one pitch, whereas dT_{25} only increases the number of thymines being in stacking with the tube (up to 15), and the number of thymines in self-stacking is still significant (Table 1). As for purine oligonucleotides, the number of their bases stacked with the tube becomes higher (14 bases for 20 ns). By 30 ns the energy of the interaction between SWCNT and dC_{25} reaches the maximum with 20 cytosines stacked with the tube, and during the following 20 ns this energy does not change practically (Figure 2). After 30 ns, 18 thymines of dT_{25} are in stacking with the tube surface and the polymer is wrapped, and there is no loop, though 3 dimers can be observed. The situation with purine oligonucleotides is different: the number of bases stacked with the tube increases with time, but oligonucleotides are not wrapped around the nanotube, and the formation of the loop is characteristic of them. The number of adenines stacked with the tube after 30 ns (16 bases) does not change up to 50 ns as well as the interaction energy (Figure 2). However, for the same time the number of guanines stacked with the tube in $d(G)_{25}$ rises gradually and reaches 17 by 50 ns. Nevertheless, after 50 ns, the polymer does not form the pitch too. Up to 45 ns, dT_{25} reaches the energy-favorable conformation on the nanotube and the number of thymines stacked with the tube runs up to 22 (more than for dC_{25}). This is accompanied by the energy increase the value of which for SWCNT: dT_{25} is by ~ 25 kcal/mol higher than that for SWCNT: dC_{25} . Up to 50 ns interaction energies between $d(A)_{25}$ or $d(G)_{25}$ and the tube become even equal which is turned out by ~ 20 kcal/mol lower than for SWCNT: dC_{25} . A lower rate of the binding energy increase of the purine oligonucleotides with the tube surface and their unwrapping of SWCNT are caused by a higher self-stacking energy than that in pyrimidine ones.⁴⁰ A stable ordering self-stacking structure of the polymer prevents its structural reorientation which needs to take the energy-favorable conformation on the tube surface.

It should be noted that the mean energy of the interaction between one nucleotide and the nanotube obtained in our simulation is about 13–15 kcal/mol (Figure 2). This value correlates with 15–18 kcal/mol evaluated earlier by Martin et al.²⁰ or with ~ 13 kcal/mol obtained by Jonson et al.¹⁹ The nucleotide–nanotube binding energy is equal to the difference of two sums.²⁴ The first of them is determined by the stacking energy of nucleotide–nanotube (vdW interaction) and water–water interaction which appeared because of decreasing the hydrophobic surface after binding of hydrophobic base of the nucleotide with the hydrophobic nanotube surface. The second one is a result of water–nanotube and water–nucleotide interactions. Fulfilled recently, the estimation of the binding energy of the nitrogen base with the nanotube showed²⁴ that the value of this energy is determined as the decreasing value of the stacking energy by about 3 kcal/mol through the solvation effect. Our evaluation of the interaction energy of one nucleotide and its base with nanotube (vdW interaction) showed that base–nanotube stacking energy gives $\sim 60\%$ contribution to the interaction energy of one nucleotide with the nanotube. As other components of the nucleotide (ribose and phosphate group) are more hydrophilic than hydrophobic, and as they do not contact with the nanotube surface directly, we believe that the solvation effect for these components is not essential. Thus, through the identity of the binding energy

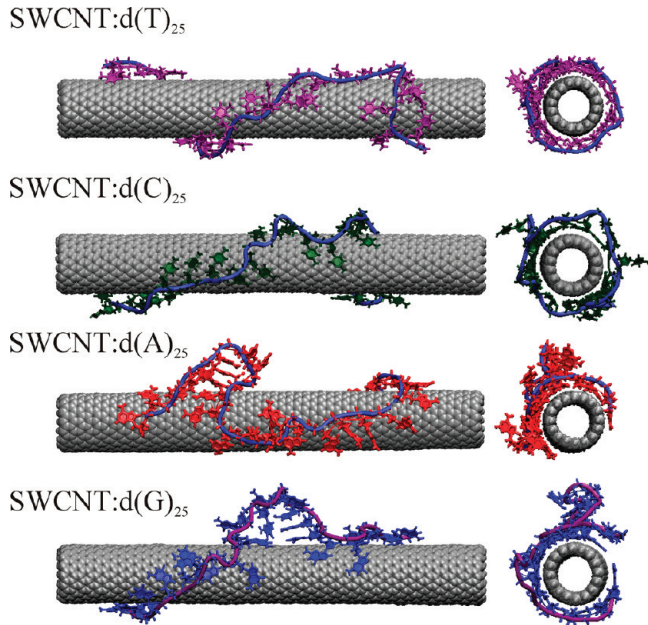


Figure 3. Snapshots of hybrids formed by nanotube (16,0) with oligonucleotides $d(T)_{25}$, $d(C)_{25}$, $d(A)_{25}$, and $d(G)_{25}$ after 50 ns simulation.

between the polynucleotide and SWCNT with vdW energy, in our case we received the overestimated value of the binding energy, which, however, is no more than by 15%.

Snapshots of hybrids formed by the (16,0) nanotube and ($d(T)_{25}$, $d(C)_{25}$, $d(A)_{25}$, and $d(G)_{25}$) oligonucleotides by 50 ns simulation are shown in Figure 3. As follows from this figure, pyrimidine oligonucleotides form a pitch around the tube with a tight covering. However, purine oligonucleotides adsorb to one side of the nanotube surface, and the strand forms a loop detached from the SWCNT side wall.

Thus, of all the oligonucleotides, dC_{25} wraps around the tube more quickly (for 20 ns) than dT_{25} which took 30 ns. Nevertheless, the number of thymines stacked with the tube to 50 ns is the greatest, and this provides the maximum binding energy of this oligonucleotide to the tube. Purine oligonucleotides do not wrap around the nanotube even for 50 ns because of the strong self-stacking energy which induces the loop formation. The loop does not disappear during the whole simulation time.

Loops formed during oligonucleotide adsorption on the tube surface retard their wrapping around SWCNT, and this limitation is manifested greatly in the case of the purine oligonucleotides. The loops can be of two types: the loop 1, when nitrogen bases of two opposite parts of the strand are in stack (see for example SWCNT: $d(A)_{25}$ in Figure 3), and this loop is formed easier by the flexible polymer; the loop 2 when self-stacked bases of two opposite parts of the strand form hydrogen bonds between them (see for example SWCNT: $d(G)_{25}$ in Figure 3). Because of steric conditions, the loop 1 should be short as the neighboring base of one part of the strand must be unfolded to allow stacking of the base from the opposite part of the strand. During simulation, dT_{25} forms such a loop which disappears by 30 ns. The loop 2 is a more stable formation as it requires a lesser distortion of the oligonucleotide without the steric limitation mentioned. The loop stability depends on the energy of the base self-stacking, hydrogen bonding inside the loop and the interaction energy of bases with the tube surface. The significance of the last energy is manifested when the

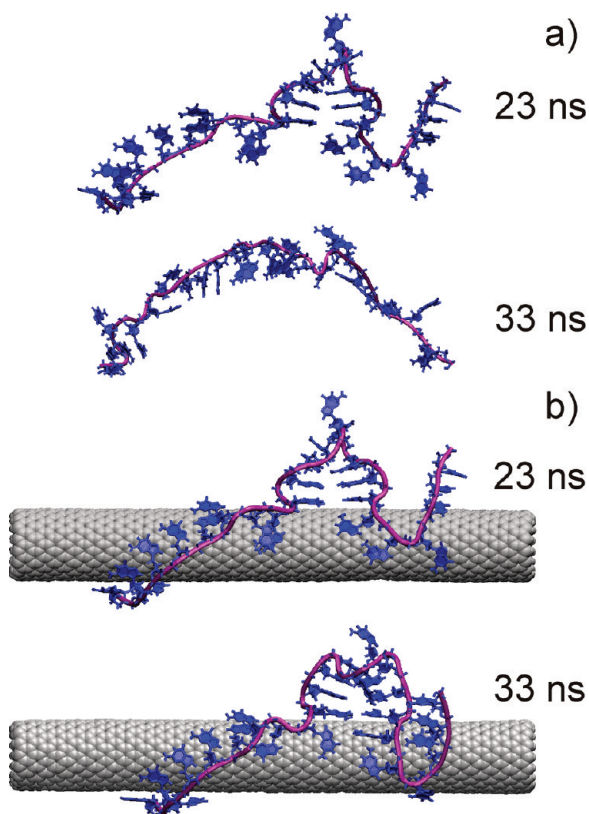


Figure 4. Snapshots of $d(G)_{25}$ adsorbed to the tube surface spontaneously: (a) after 23 ns simulation (the nanotube was extracted) (upper) and of this oligonucleotide (lower) after next 10 ns simulation without the nanotube; (b) after 23 ns simulation (upper) and after 33 ns (lower).

loop begins to contact with the tube surface through the bases at the beginning/end of this loop. These bases serve as anchors keeping the loop. It should be noted that the energy of the base adsorption on the nanotube^{39,41} is higher than that of the base self-stacking energy.⁴⁰ Therefore, desorption of these bases from the tube surface can occur after self-stacking destruction. Ab initio calculation shows that the energy of purine base self-stacking⁴⁰ as well as their energy adsorption onto the nanotube⁴¹ is stronger than that for pyrimidine one. Therefore, such a loop is especially stable in the case of the purine oligonucleotides hindering these polymers to wrap around the nanotube. The stable loop is an additional factor making difficult the purine polymer wrapping around the nanotube. To verify the important role of anchor bases at the beginning/end of this loop, we observed the alteration of the loop when the tube was extracted from the box and the interaction of the oligonucleotide with the nanotube was excluded. For this purpose dG_{25} which formed the loop on SWCNT surface after 20 ns simulation was selected (Figure 4).

After this procedure, the loop practically disappeared in the next 10 ns (Figure 4a) while in the tube's presence it was kept not only after 10 ns (Figure 4b) but during the following 30 ns at the least (the observation is limited with the maximal simulation time) (Figure 3).

Estimations obtained from modeling allowed us to establish the oligonucleotide row which demonstrates decreasing of interaction energies between them and the carbon nanotube: $d(T)_{25} > d(C)_{25} > d(A)_{25} \approx d(G)_{25}$.

3.2. Temperature Influence on Spontaneous Adsorption of Oligonucleotides on SWCNT Surface.

As the base self-

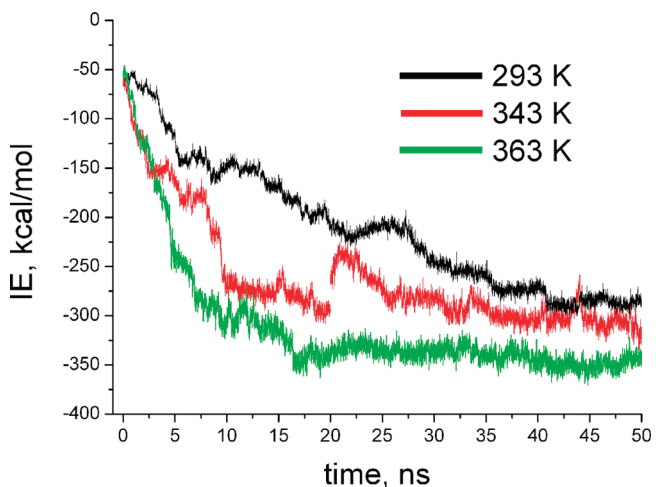


Figure 5. Dependence of interaction energy between SWCNT and $r(C)_{25}$ on simulation time at 293, 343, and 363 K.

stacking hinders the spontaneous adsorption of the oligonucleotide onto the nanotube surface, the temperature must have an appreciable effect on the rate of oligonucleotide to occupy the more energetically favored conformation on the nanotube. It is well studied that the temperature rise leads to the helix–coil transition of DNA⁴² (the so-called DNA melting). Some estimations of the competition between the base self-stacking and their adsorption on the carbon nanotube surface can be obtained from the comparison of magnitudes of their energies. As these energies for hybrids in water are unknown, certain information can be obtained from the comparison of the base adsorption onto the nanotube surface⁴¹ and their self-stacking energies⁴⁰ determined by ab initio method. From these calculations, the following energies were obtained: 16 and 11.3, 14 and 8.8, and 12 and 8.3 kcal/mol for guanine, adenine, and cytosine, respectively. It means that the adsorption energy of nitrogen bases on the tube surface is by 4–5 kcal/mol higher than the energy of their self-stacking.

The temperature influence on the spontaneous adsorption of oligonucleotides on the SWCNT surface will be manifested in two different effects. On the one hand, the temperature rise breaks the base self-stacking, and the polymer becomes more flexible and disposed to reorientation of the strand structure. Thus, the oligonucleotide increases the rate of achieving the energy-favorable conformation on the nanotube to provide the maximum magnitude of the binding energy with the tube. Temperature provides the energetically more favorable position of the polymer on the nanotube in a shorter time when more bases are stacked with the nanotube surface. At the same time the temperature rise makes easier the barrier overcoming between neighboring hexagons. This promotes the movement of the base along the nanotube surface and permits the polymer to occupy an energetically more favored contact with the SWCNT surface. On the other hand, it is necessary to take into account the base desorption from the nanotube surface, which increases with the temperature rise too. At higher temperature, bases should move away from the tube. Desorption of the polymer with increasing temperature has been observed experimentally.⁴³ Evidently, temperatures used in our simulation of the SWCNT: $r(C)_{25}$ hybrid formation (293, 343, and 363 K) are not enough to provide the effective base desorption from the nanotube surface (Figure 5).

However, under these temperatures the polymer order → disorder transition takes place.⁴² It should be noted that noticeable desorption of poly(rA) from the nanotube was not also observed in our UV-absorption spectroscopy study of SWCNT:poly(rA) suspension⁷ when it was heated from room temperature up to 363 K. Just in this temperature range the adsorption of r(C)₂₅ on the tube surface was simulated. Figure 5 presents dependence of the interaction energy in the SWCNT:r(C)₂₅ hybrid as a function of time at three temperatures. As the Figure shows, temperatures have an essential influence on the rate of achieving the energetically more favored conformation on the

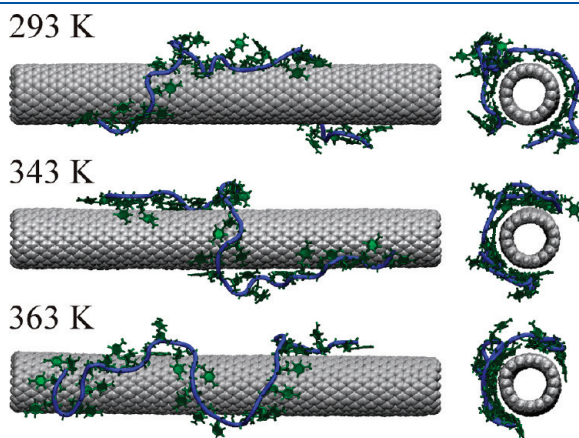


Figure 6. Snapshots of SWCNT:r(C)₂₅ obtained after 50 ns simulation at 293, 343, and 363 K.

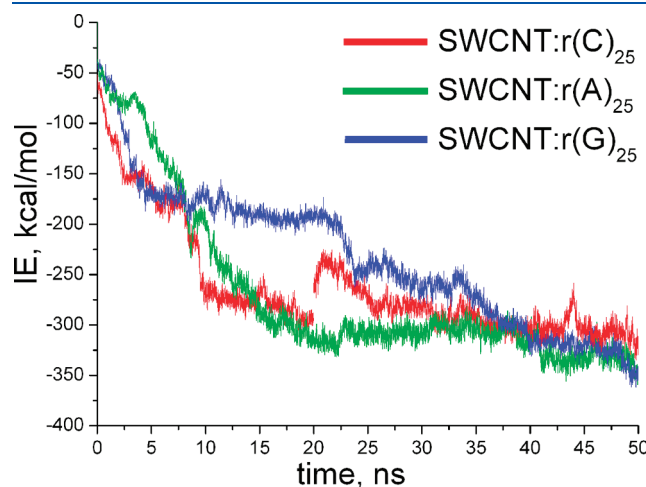


Figure 7. Dependence of interaction energy between SWCNT and r(C)₂₅, r(A)₂₅, and r(G)₂₅ oligonucleotide on simulation time at 343 K.

nanotube, which is reached for 20 ns at 363 K and for twice as long at 343 K. At 293 K this rate is very slow: so, for 50 ns only 16 cytosines are stacked with the tube surface, a loop is formed on the tube (Figure 6) and the oligonucleotide does not achieve the stable conformation on the tube surface even for 50 ns.

Figure 6 demonstrates snapshots of SWCNT:r(C)₂₅ hybrid after 50 ns simulation obtained at 293, 343, and 363 K. As can see from these snapshots, r(C)₂₅ acquires U-shaped form on the SWCNT surface at 363 K with 20 cytosines stacked with the tube. At 343 K the number of cytosines stacked with the tube is less by one.

3.3. Comparison of Deoxi- and Ribooligonucleotides Abilities for Adsorption onto Carbon Nanotube. When studying effects of the polymer structure upon its adsorption onto the nanotube, it is interesting to compare deoxy- and ribooligonucleotides having the same bases. These polymers differ in the additional hydroxyl group appearing in the ribose ring (in the second position) of the ribooligomer. As a result, the ribose structure in RNA becomes more rigid, in comparison with the DNA one. In RNA ribose takes only C3'-endo conformation, and this permits the 2'-OH group to avoid its impact on H-C8 of purines and H-C6 of pyrimidines in the nitrogen base attached. In A-RNA helical structure an interaction between hydrogen of H2' of ribose and O4' of the neighboring residue can occur. Because of the additional hydroxyl group in ribose, some conformations being available for DNA become inaccessible for RNA. On the other hand, the additional hydroxyl group restricts the number of hydrogen-bonding sites, and this can give RNA possibilities for specific interactions.⁴⁴ We note that, as was simulated recently, the stiff and flexible polymer has different tendencies to wrap around the SWCNT.^{45,46}

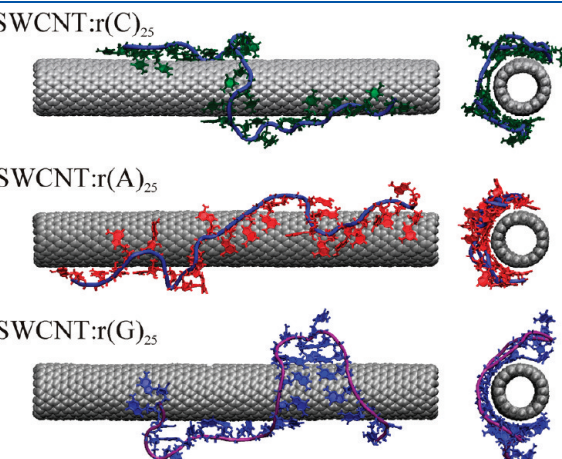


Figure 8. Snapshots of hybrids formed by nanotube (16,0) with r(C)₂₅, r(A)₂₅, and r(G)₂₅ oligonucleotides after 50 ns simulation.

Table 2. Number of Nitrogen Bases of Following Oligonucleotides: r(C)₂₅, r(A)₂₅, and r(G)₂₅ Which Were in Stack with Tube Surface and Self-Stacked for Different Simulation Times

time (ns)	type of nitrogen base stacking	r(C) ₂₅	r(A) ₂₅	r(G) ₂₅
10	stacked with tube	13 cytosines	9 adenines	5 guanines
	self-stacking	1 (CCCC)	1 (AAA), 2 (AA)	1 (GGGGGGGG), 1 (GGGG), 1 (GGG), loop
30	stacked with tube	16 cytosines	15 adenines	7 guanines
	self-stacking	1 (CC), loop	3 (AA)	1 (GGGGGGGG), 2 (GGG), 1 (GG), loop
50	stacked with tube	19 cytosines	18 adenines	16 guanines
	self-stacking	loop	1 (AA)	2 (GG), loop

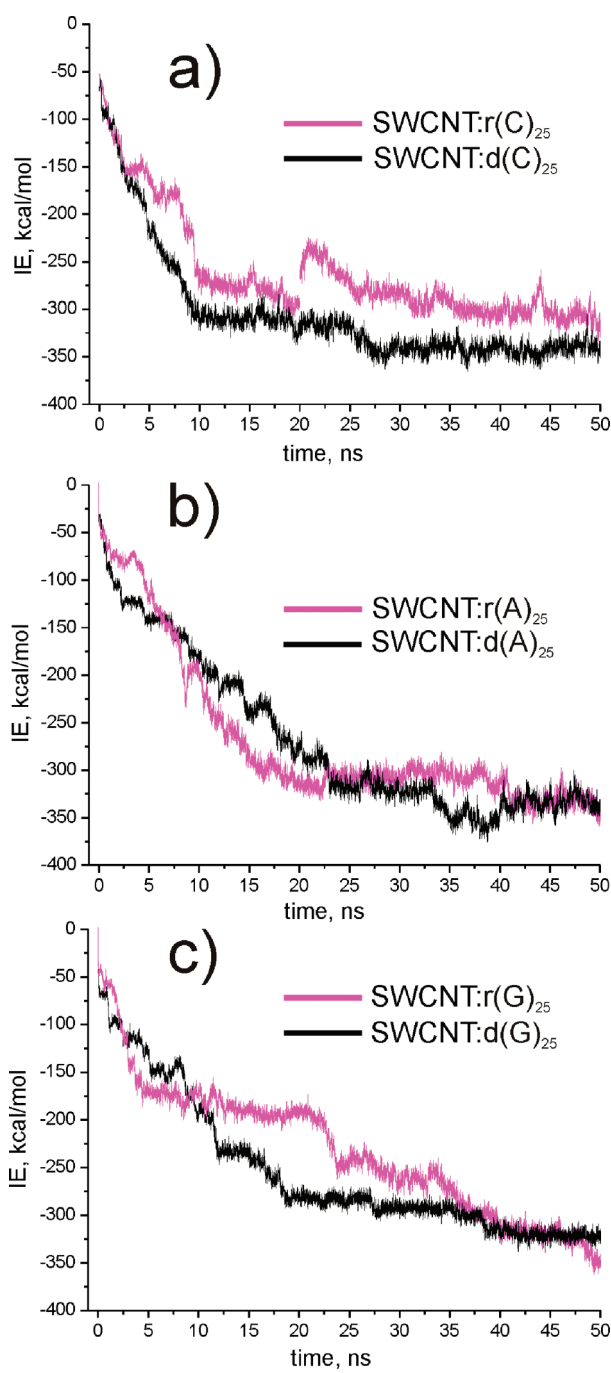


Figure 9. Dependence of interaction energy between SWCNT and $r(C)_{25}$ or $d(C)_{25}$ (a), $r(A)_{25}$ and $d(A)_{25}$ (b), and $r(G)_{25}$ and $d(G)_{25}$ (c) oligonucleotides on simulation time at 343 K.

We simulated the process of the adsorption onto the tube surface of the following homoribooligonucleotides: $r(C)_{25}$, $r(A)_{25}$, and $r(G)_{25}$. Dependence of the interaction energy of these oligonucleotides with SWCNT on simulation time is shown in Figure 7. As Figure shows, oligomers demonstrate different adsorption rates and different binding energies at the end of the simulation time. As for deoxyoligonucleotides, the pyrimidine oligomer $r(C)_{25}$ shows higher rate, especially during the first 10 ns. After 10 ns simulation, the oligomer does not make a helical pitch around the tube, and only 13 cytosines are stacked with the nanotube surface (Table 2.).

During subsequent modeling time, the number of cytosines stacked with the nanotube surface increases, reaching 19 to 40 ns. But, as before, $r(C)_{25}$ does not wrap around the nanotube and forms a loop which does not disappear even to 50 ns. Between 20 and 30 ns of simulation time, the oligomer changes its conformation relatively to the nanotube, and, as a result, its binding energy lowers by about 50 kcal/mol. During the subsequent 5 ns, this energy decrease is compensated by a new more energetically favored conformation.

Purine oligonucleotides show a lower rate of their adsorption on the tube; $r(A)_{25}$ stands out among these oligomers, which to 20 ns has the most interaction energy among all ribooligonucleotides with 16 adenines stacked with the tube. At the same time, $r(A)_{25}$ does not wrap around the nanotube, a loop is not formed yet, and only one trimer and one dimer can be observed in the structure of this oligomer. As before, by 50 ns the oligomer is not wrapped too, and the rise of the binding energy is caused mainly by the increase of the quantity of adenines stacked with the tube, which reaches 18 at the end of the simulation time. As well, by 50 ns the interaction energy between components of SWCNT: $r(G)_{25}$ hybrid is about of the same magnitude, and 16 guanines are stacked with the tube. However, $r(G)_{25}$ is not wrapped around the tube and forms a loop, as shown in Figure 8. Stronger binding energy of the pyrimidine homoribopolynucleotide with the tube surface than of the purine one is confirmed by the hypochromic effect which becomes apparent in the decrease of UV-visible light absorption by SWCNTs hybrid formed with poly(rC) and poly(rG), in comparison with SWCNT:SDS.⁴⁷

It is worthwhile to compare directly spontaneous adsorption of two oligonucleotides with identical bases but differing in ribose. Figure 9a presents interaction energies of the nanotube with $d(C)_{25}$ and $r(C)_{25}$ as a function of the simulation time. It is seen from the Figure that the adsorption rate of the first oligonucleotide on the tube is higher, and the energy of $r(C)_{25}$ binding with the nanotube is lower than that for $d(C)_{25}$, and this oligonucleotide does not wrap around SWCNT.

The situation with other oligonucleotide pairs $d(A)_{25}$ and $r(A)_{25}$ is different (Figure 9b). The noticeable difference in the dependence of energies of the nanotube:oligomer binding is not observed; both of them do not wrap around the tube. In spite of different rates of $d(G)_{25}$, $r(G)_{25}$ adsorption on the nanotube surface their binding energies are of about the same value in the end of simulation (Figure 9c). These oligomers do not make the pitch around the tube too, and their strands form loops on the tube surface.

4. CONCLUSIONS

The simulation of the spontaneous adsorption of homooligonucleotides (dC_{25} , dT_{25} , dG_{25} , dA_{25}) onto the surface of the carbon nanotube by the molecular dynamics method demonstrated that pyrimidine oligonucleotides can wrap around the nanotube for 20–30 ns at 343 K. At the same time, purine oligonucleotides do not make the complete pitch around the nanotube even after 50 ns. Such a behavior is caused with a stronger energy of self-stacking between bases of purine oligomers than that of pyrimidine ones, which prevents their structural reorientation that is necessary for occupation of the most energetically favored conformation on the nanotube surface. The initial adsorption rate is higher for dC_{25} but dT_{25} interaction with the nanotube surface at the end of simulation time (50 ns) becomes stronger as a larger number of thymines is in stacking with the

nanotube. Estimations obtained from modeling allowed us to establish the oligonucleotide row $d(T)_{25} > d(C)_{25} > d(A)_{25} \approx d(G)_{25}$ which demonstrates a decrease in the interaction energy between the oligomer and the carbon nanotube.

The loops formed during oligonucleotides adsorption on the tube surface hinder their wrapping around the tube, and this limitation is manifested greatly in the case of purine oligonucleotides. The bases contacted with the tube surface at the beginning/end of the loop play a significant role in the keeping of this conformation because they serve as anchors for this loop.

It was shown that temperature growth increases the rate of the oligonucleotides to reach the maximum of the binding energy mainly due to the destruction of nitrogen base self-stacking. As a result, this makes the process of the oligomer wrapping around the nanotube easier.

Ribonucleic oligomers $r(C)_{25}$, $r(A)_{25}$, and $r(G)_{25}$ do not make the pitch around the nanotube even for 50 ns. The additional hydroxyl group in the ribose lowers both the rate of spontaneous oligomer adsorption and the possibility of its wrapping as well. The presence of the additional hydroxyl group in ribose restricts the conformational flexibility of ribooligonucleotides in comparison with their deoxy analogues, which reduces the possibility of the rapid occupation of energetically favored conformation on the nanotube surface.

The obtained results offer the challenge for practical use of pyrimidine deoxyoligonucleotides for solubilization of carbon nanotubes in water during moderate temperature heating (in the temperature range up to 100 °C).

AUTHOR INFORMATION

Corresponding Author

*E-mail: karachevtsev@ilt.kharkov.ua.

ACKNOWLEDGMENT

We are grateful to Dr. S. G. Stepanian for helpful discussion and Dr. L. F. Belous for useful consultation at all simulation stages. This work was partially supported by Grants of the Science and Technology Center in Ukraine and National Academy of Science of Ukraine (N 4950). As well, the authors acknowledge the Computational Center at B. I. Verkin Institute for Low Temperature Physics and Engineering for providing computer time.

REFERENCES

- (1) O'Connell, M. J.; Boul, P.; Ericson, L. M.; Huffman, Ch.; Wang, Y.; Haros, E.; Kuper, C.; Tour, J.; Ausman, K. D.; Smalley, R. E. *Chem. Phys. Lett.* **2001**, *342*, 265–271.
- (2) Zheng, M.; Jagota, A.; Semke, E.; Diner, B.; Mclean, R.; Lustig, S.; Richardson, R.; Tassi, N. *Nat. Mater.* **2003**, *2*, 338–342.
- (3) Zheng, M.; Jagota, A.; Strano, M.; Santos, A.; Barone, P.; Chou, S.; Diner, B.; Dresselhaus, M.; Mclean, R.; Onoa, G.; Samsonidze, G.; Semke, E.; Usrey, M.; Walls, D. *Science* **2003**, *302*, 1545–1548.
- (4) Keren, K.; Berman, R. S.; Buchstab, E.; Sivan, U.; Braun, E. *Science* **2003**, *302*, 1380–1382.
- (5) Gigliotti, B.; Sakizie, B.; Bethune, D. S.; Shelby, R. M.; Cha, J. N. *Nano Lett.* **2006**, *6*, 159–164.
- (6) Zhao, W.; Gao, Y.; Brook, M. A.; Li, Y. *Chem. Commun.* **2006**, *34*, 3582–3584.
- (7) Karachevtsev, V. A.; Gladchenko, G. O.; Karachevtsev, M. V.; Valeev, V. A.; Leontiev, V. S.; Lytvyn, O. S. *Chem. Phys. Phys. Chem.* **2008**, *9*, 2872–2881.
- (8) Tu, X.; Manohar, S.; Jagota, A.; Zheng, M. *Nature* **2009**, *460*, 250–253.
- (9) Burghard, M.; Klauk, H.; Kern, K. *Adv. Mater.* **2009**, *21*, 2586–2600.
- (10) *Carbon Nanotube Electronics*; Javey, A., Kong, J., Eds.; Springer: New York, 2008.
- (11) Yarotski, D. A.; Kilina, S. V.; Talin, A. A.; Tretiak, S.; Prezhdo, O. V.; Balatsky, A. V.; Taylor, A. J. *Nano Lett.* **2009**, *9*, 12–17.
- (12) Star, A.; Tu, E.; Niemann, J.; Gabriel, J. P.; Joiner, C. S.; Valcke, C. *Proc. Natl. Acad. Sci. U.S.A.* **2006**, *103*, 921–926.
- (13) Jeng, E. S.; Moll, A. E.; Roy, A. C.; Gastala, J. B.; Strano, M. S. *Nano Lett.* **2006**, *6*, 371–375.
- (14) Gao, H.; Kong, Y.; Cui, D.; Ozkan, C. S. *Nano Lett.* **2003**, *3*, 471–473.
- (15) Gao, H.; Kong, Y. *Annu. Rev. Mater. Res.* **2004**, *34*, 123–150.
- (16) Lu, G. P.; Maragakis, P.; Kaxiras, E. *Nano Lett.* **2005**, *5*, 897–900.
- (17) Manohar, S.; Tang, T.; Jagota, A. *J. Phys. Chem. C* **2007**, *111*, 17835–17845.
- (18) Zhao, X.; Johnson, J. K. *J. Am. Chem. Soc.* **2007**, *129*, 10438–10445.
- (19) Johnson, R. R.; Johnson, A. T. C.; Klein, M. L. *Nano Lett.* **2008**, *8*, 69–75.
- (20) Martin, W.; Zhu, W.; Krilov, G. *J. Phys. Chem. B* **2008**, *112*, 16076–16089.
- (21) Frischknecht, A. L.; Martin, M. G. *J. Phys. Chem. C* **2008**, *112*, 6271–6278.
- (22) Kim, S. N.; Kuang, Z.; Grote, J. G.; Farmer, B. L.; Naik, R. R. *Nano Lett.* **2008**, *8*, 4415–4420.
- (23) Johnson, R. R.; Kohlmeyer, A.; Johnson, A. T. C.; Klein, M. L. *Nano Lett.* **2009**, *9*, 537–541.
- (24) Johnson, R. R.; Johnson, A. T. C.; Klein, M. L. *Small* **2010**, *6*, 31–34.
- (25) Roxbury, D.; Manohar, S.; Jagota, A. *J. Phys. Chem. C* **2010**, *114*, 13267–13276.
- (26) Karplus, M.; McCammon, J. A. *Nat. Struct. Biol.* **2002**, *9*, 646–652.
- (27) Gladchenko, G. O.; Karachevtsev, M. V.; Leontiev, V. S.; Valeev, V. A.; Glamazda, A. Yu.; Plokhotnichenko, A. M.; Stepanian, S. G. *Mol. Phys.* **2006**, *104*, 3193–3201.
- (28) Heller, D. A.; Jeng, E. S.; Yeung, T. K.; Martinez, B. M.; Moll, A. E.; Gastala, J. B.; Strano, M. *Science* **2006**, *311*, 508–511.
- (29) Nakashima, N. *Sci. Technol. Adv. Mater.* **2006**, *7*, 609–616.
- (30) Xu, Y.; Pehrsson, P. E.; Chen, L.; Zhang, R.; Zhao, W. *J. Phys. Chem. C* **2007**, *111*, 8638–8643.
- (31) Cathcart, H.; Nicolosi, V.; Hughes, J. M.; Blau, W. J.; Kelly, J. M.; Quinn, S. J.; Coleman, J. N. *J. Am. Chem. Soc.* **2008**, *130*, 12734–12744.
- (32) Karachevtsev, M. V.; Lytvyn, O. S.; Stepanian, S. G.; Leontiev, V. S.; Adamowicz, L.; Karachevtsev, V. A. *J. Nanosci. Nanotechnol.* **2008**, *8*, 1473–1480.
- (33) Jeng, E. S.; Barone, P. W.; Nelson, J. D.; Strano, M. S. *Small* **2007**, *3*, 1602–1609.
- (34) Phillips, J. C.; Braun, R.; Wang, W.; Gumbart, J.; Tajkhorshid, E.; Villa, E.; Chipot, Ch.; Skeel, R. D.; Kale, L.; Schulten, K. *J. Comput. Chem.* **2005**, *26*, 1781–1802.
- (35) Foloppe, N.; MacKerell, A. D., Jr. *J. Comput. Chem.* **2000**, *21*, 86–104.
- (36) Humphrey, W.; Dalke, A.; Schulten, K. *J. Mol. Graphics* **1996**, *14*, 33–38.
- (37) Neidle, S. *Principles of Nucleic Acid Structure*; Academic Press: London, 2008.
- (38) Meng, S.; Maragakis, P.; Papaloukas, C.; Kaxiras, E. *Nano Lett.* **2007**, *7*, 45–50.
- (39) Enyashin, A. N.; Gemming, S.; Seifert, G. *Nanotechnology* **2007**, *18*, 245702 (1–10).
- (40) Sponer, J.; Leszczynski, J.; Hobza, P. *Biopolymers* **2002**, *61*, 3–31.

- (41) Stepanian, S. G.; Karachevtsev, M. V.; Glamazda, A. Yu.; Karachevtsev, V. A.; Adamowicz, L. *J. Phys. Chem. A* **2009**, *113*, 3621–3629.
- (42) Cantor, C. R.; Schimmel, P. R. *Biophysical Chemistry. Part II*; W. H. Freeman & Co.: San Francisco, 1980.
- (43) Tang, B. Z.; Xu, H. Y. *Macromolecules* **1999**, *32*, 2569–2576.
- (44) Bloomfield, V. A.; Crothers, D. M.; Tinoco, I., Jr. *Nucleic Acids. Structures, Properties and Functions*; University Science Books: Sausalito, CA, 2000.
- (45) Tallury, S. S.; Pasquinelli, M. A. *J. Phys. Chem. B* **2010**, *114*, 4122–4129.
- (46) Tallury, S. S.; Pasquinelli, M. A. *J. Phys. Chem. B* **2010**, *114*, 9349–9355.
- (47) Karachevtsev, V. A.; Plokhotnichenko, A. M.; Karachevtsev, M. V.; Leontiev, V. S. *Carbon* **2010**, *48*, 3682–3691.